MENOUFIYA UNIVERSITY
FACULTY OF ENGINEERING
ENG. RESEARCH BULL.
Vol.17 part 2, 1994

P.P. : 69 : 85
Received at :17/7/1994
Accepted at :10/8/1994

AN IDEALLY COMMUTATED SWITCHED RELUCTANCE MOTOR DRIVE

M.M.Khater[‡], M.M.El-Shanawany[‡], A.A.Hassanein[‡] and B.W.Williams[‡‡]

[‡] *Department of Electrical Engineering, Faculty of Engineering, Menoufiya University, Shebin El-Kom, Egypt*
[‡‡] *Department of Computing & Electrical Engineering, Heriot-Watt University, Edinburgh EH14 4AS, United Kingdom*

ABSTRACT

Although various excitation current waveforms are possible, there is only an ideal one which maximizes the output torque of a switched reluctance motor(SRM). This paper presents an analytical and experimental study to characterize this ideal current waveform for a multiphase machine. Throughout this study the commutation process is analyzed and an ideal commutation angle is obtained for each running condition. A simple procedure is given to predict this angle and incorporated in a larger computer program to study its relation with the motor speed and its interaction with the drive performance. The analytical results are verified experimentally on a five-phase SRM.

1. INTRODUCTION

Switched reluctance motors (SRMs) have been seriously considered as a promising competitor to inverter driven induction motors. The extremely simple and rugged construction of both the motor and its electronic power converter are among many potential advantages of this new machine[1]. In its basic form, a SRM consists of a singly excited, doubly salient structure of steel laminations fed with a switched dc pulses through an electronic power converter in a closed loop configuration. A rotor position sensor is essiential to generate the converter drive signals and commutate phase excitation pulses[2].

Being a salient pole machine, the phase inductance of a SRM varies between a minimum and a maximum value at unaligned and aligned axes respectively. For its motor operation, each phase current pulse has to be switched-on, at some point before the rising inductance and it has to be decreased to zero before decreasing the inductance[3]. Figure(1) shows a typical phase current pulse along with an ideal phase inductance profile. This pulse can be divided into three main subsequent periods namely; rising angle

θ_r, commutation angle θ_c and fall angle θ_f. These angles can be adjusted to many different values but there is always an ideal value for each one which maximizes the output torque.

In spite of the revival interest of SRMs, a little work has been reported, in literature, about their excitation current waveform and its interaction with the machine performance. One of these early studies is the work of *Ray et al*[2] in which the current waveform is used to optimize the performance/cost ratio for three and four phase SRM. The torque per rms excitation current is used to characterise an optimum current waveform with different mark-space ratios for a 3-phase 12/8 machine, *Finch et al*[4]. A mathematical model for this waveform is developed for stationary rotor[5] and rotating machine[6], to find out its rate of change and peak value for both conditions. In these studies phase current waveform is always analyzed without a direct relation to poles or gap geometries. In[3] poles geometry and phase inductance parameters at both extreme rotor positions are used to find out the power converter rating for certain machine parameters. Most of the former studies considered either a three or four phase machine with no restrictions on their power converters and phase currents were always treated independently. It is not always true that the excitation current waveform can be analyzed irrespective of the power converter circuit type. With a multiphase machine, where it becomes necessary to reduce the total number of converter switching devices[7], the waveform is highly converter-dependant. An accurate analysis of this waveform should take into account the power converter type and its restrictions on the commutation process.

In the present study the phase current waveform of a multiphase SRM fed with a *compact power converter* circuit is analyzed. The detailed description of this circuit is found in[9]. On its basis, it is always possible to build-up a unipolar converter with a number of switches equals the number of phases plus one. A single switch is usually shared by two phases and consequently it has to serve their switching requirements. A general section of this converter is shown in figure(2).

The purpose of this paper is to lay out the ideal specifications of the excitation current waveform for a multiphase SRM which maximizes its average torque. This waveform is mainly specified by its *rise*, *commutation* and *fall* angles and their coincidence with the inductance profile for each phase. An analytical study is given and experimentally verified on a five-phase SRM.

2. ANALYSIS OF EXCITATION PULSES:

A general waveform of the applied voltage across the phase winding for each current pulse under chopping is shown in figure(3). The current waveform is also shown on the same figure. The existence of some periods depends on the motor speed and machine physical dimensions.

For motor operation of a switched reluctance machine, each phase

has to be switched-on at some point before the rising inductance. At very low speed, the back emf would not be sufficient to limit the current and it will rapidly increase. This current should be modulated and maintained at certain level within winding rating. By increasing the motor speed there is a *base speed*, ω_b at which the back emf would be sufficient to maintain a flat-topped current without any chopping[3]. The base speed for a given current can be obtained from the flux linkage current characteristics of the machine. The trajectory of one current-flux linkage pulse is shown in Fig.(4). Along AB flux linkage rises from ψ_{min} to ψ_{max} by the movement of one rotor pole from full unaligned to full aligned position at constant phase current of magnitude I. Since the unaligned characteristics are usually linear then,

$$\psi_{min} = L_o I \tag{1}$$

The time taken to move the rotor pole from A to B is given by,

$$t_{AB} = \frac{\beta_s}{\omega} \tag{2}$$

If the current is maintained constant along AB, then the rise in flux linkage is given by;

$$\psi_{max} - \psi_{min} = (V_s - IR)\, t_{AB} \tag{3}$$

Substituting the value of t_{AB} from Eqn(2) in Eqn(3), the rise in flux linkage can be rewritten as;

$$\psi_{max} - \psi_{min} = (V_s - IR)\, \frac{\beta_s}{\omega} \tag{4}$$

If this flux linkage rise is obtained at the constant current I, without any chopping, the motor speed is its base speed which can be expressed as;

$$\omega_b = \frac{(V_s - IR)\, \beta_s}{\psi_{max} - \psi_{min}} \tag{5}$$

For any higher speed, the back emf is high enough to limit the phase current without chopping.

To maximize machine output torque, excitation current waveform should satisfy the following two conditions;

1. It should be raised to its maximum value just as the inductance of the winding starts to increase (i.e. early turn-on), that is;

$$i(\theta)\big|_{\theta_r} = I \tag{6}$$

2. It should be maintained as long as possible without producing any negative torque. In other words, it should satisfy the following condition;

$$\theta_c + \theta_f = \beta_r \tag{7}$$

If the winding ohmic resistance is neglected, the rise angle can

be expressed as Eqn(8), which satisfies the first condition.

$$\theta_r = \frac{\omega L_o I}{V_s} \qquad (8)$$

Commutation and fall angles are related to each other as stated by Eqn(7). It is sufficient to obtain one of them to predict the other. For its importance, the commutation angle will be obtained for different running conditions. Before going-on, the average excitation voltage during chopping periods is required for the later analysis.

At any speed ω below the base speed, phase current is maintained at constant magnitude I by chopping the applied voltage V_s to an average value V_c which satisfies Eqn(4),

$$\psi_{max} - \psi_{min} = (V_c - IR)\frac{\beta_s}{\omega} \qquad (9)$$

An expression for V_c can be obtained from Eqns(5) and (9) as follows;

$$V_c = V_s\left(\frac{\omega}{\omega_b}\right) + IR\left(1 - \frac{\omega}{\omega_b}\right) \qquad (10)$$

If the winding resistance is neglected, eqn(10) can be rewritten in the following simplified form;

$$V_c = \left(\frac{\omega}{\omega_b}\right).V_s \qquad (11)$$

After commutation, the last phase would see a modulated negative voltage with an average value V_{alt} which can be expressed by either of the following alternative forms;

$$V_{alt} = V_s - V_c \qquad (12)$$

$$V_{alt} = \left(1 - \frac{\omega}{\omega_b}\right).V_s \qquad (13)$$

3. PREDICTION OF THE IDEAL COMMUTATION ANGLE:

The ideal commutation angle for a particular current and speed can be predicted by ensuring that the rise of flux linkage to its peak value is equal to the subsequent fall to zero. The following analysis applies to phase 1 (P_1) of figure(2).

3.1. Motors up to Four Phases:

In these motors the rotor pole arc usually does not exceed two step angles. It is not possible that the third phase overlaps the first one. Depending on rotor speed, the commutation process for these motors can be categorized into four different modes.

MODE 1: *Speeds below the first commutation speed* $\omega<\omega_0$:

During this mode it is possible to reduce the current in first phase to zero while the current in the next one still chopping. The switching sequence is summarised in table(1).

S / M	S_a	D_a	S_b	D_b	S_c	D_c
1.	on	off	on	off	off	off
2.	chop	chop	on	off	off	off
3.	chop	chop	on	off	on	off
4.	off	on	chop	chop	on	off

Table(1). The switching sequence at $\omega<\omega_0$

During this mode each phase is exposed to *full positive* supply voltage during current rising (sub-mode 1), *reduced positive* voltage during chopping (sub-modes 2,3) and finally *reduced negative* voltage due to chopping in the next phase (sub-mode 4). The current-flux linkage loop is shown in figure(5). The flux linkage rise along OAB equals the flux linkage fall along BCO.

$$L_o.I + c.\psi_{max} = \frac{\beta_r - c\beta_s}{\omega}.V_{neg} \qquad (14)$$

from which the commutation angle can be obtained;

$$\theta_{c3} = c\beta_s = \beta_r\left(1 - \frac{\omega}{\omega_b}\right) - \frac{\omega L_o I}{V_s} \qquad (15)$$

The upper limit of this mode is the first commutation speed ω_0 which can be obtained from eqn(15) when the commutation angle exactly equals the step angle.

$$\omega_o = \frac{\omega_b(\beta_r - t)}{\beta_r + \frac{\omega_b L_o I_m}{V_s}} \qquad (16)$$

MODE 2: *Speeds over or equal the first commutation speed and less than the second commutation speed* $\omega_0<=\omega<\omega_1$:

The commutation angle during this mode is less than one step angle such that it is necessary to turn off one switch of the first phase while the current is still rising in the second one. The switching sequence is summarised in table(2).

During this mode each phase is exposed to *full positive* supply voltage during current rising (sub-mode 1), *reduced positive* during chopping (sub-mode 2), *zero voltage* to allow the current in the next phase to rise (sub-mode 3) and finally *reduced negative* voltage due to chopping in the next phase (sub-mode 4).

M \ S	S_a	D_a	S_b	D_b	S_c	D_c
1.	on	off	on	off	off	off
2.	chop	chop	on	off	off	off
3.	off	on	on	off	on	off
4.	off	chop	chop	chop	on	off

Table(2). The switching sequence at $\omega_0 <= \omega < \omega_1$

The current-flux linkage loop is shown in figure(6). The flux linkage rise along OAB equals its fall along CDO.

$$L_o . I + c . \psi_{max} = \frac{\beta_r - c . \beta_s - \beta_{zero}}{\omega} . V_{neg} \qquad (17)$$

$$\beta_{zero} = t - c . \beta_s \qquad (18)$$

from these equations the commutation angle, during this mode, can be obtained;

$$\theta_{c4} = c\beta_s = \left(\frac{\omega_b}{\omega} - 1 \right) (\beta_r - t) - \frac{\omega_b L_o I}{V_s} \qquad (19)$$

This commutation angle is always valid while the fall angle θ_f is less than one step angle. By the increase of speed θ_f increases until it becomes exactly one step then another mode starts. The upper limit of this mode is;

$$\theta_f = t \qquad (20)$$

$$\beta_r - c . \beta_s = t \qquad (21)$$

Substituting the value of $c.\beta_s$ from eqn(21) in eqn(19), the upper limit speed, second commutation speed, of this mode can be obtained;

$$\omega_1 = \frac{\omega_b (\beta_r - t)}{2 \left(\beta_r - t + \frac{\omega_b L_o I}{2 V_s} \right)} \qquad (22)$$

MODE 3: *Speeds over or equal the second commutation speed and less than the base speed* $\omega_1 <= \omega < \omega_b$*:*

During this mode θ_f exceeds one step angle such that it is possible to apply the full negative supply voltage across the first phase just after the end of chopping period of the second phase. The switching sequence is summarised in table(3).

During this mode each phase is exposed to *full positive* supply voltage during current rising (sub-mode 1), *reduced positive* during chopping (sub-mode 2), *zero voltage* to allow the current in the next phase to rise (sub-mode 3) *reduced negative* voltage due to chopping in the next phase (sub-mode 4) and finally *full*

negative voltage when chopping no longer exists in the next phase (sub-mode 5).

M \ S	S_a	D_a	S_b	D_b	S_c	D_c	S_e	D_e
1.	on	off	on	off	off	off	off	off
2.	chop	chop	on	off	off	off	off	off
3.	off	on	on	off	on	off	off	off
4.	off	on	chop	chop	on	off	off	off
5.	off	on	off	on	on	off	on	off

Table(3). The switching sequence at $\omega_1 <= \omega < \omega_b$

The current-flux linkage loop is shown in figure(7). The flux linkage rise along OAB equals its fall along CDEO.

$$L_o I + V_s \frac{c\beta_s}{\omega_b} = \frac{\beta_{alt}}{\omega}\left(1 - \frac{\omega}{\omega_b}\right) V_s + \frac{\beta_{neg}}{\omega} V_s \qquad (23)$$

$$\beta_{alt} = c\beta_s \qquad (24)$$

$$\beta_{neg} = \beta_r - t - c\beta_s \qquad (25)$$

From these equations the commutation angle for this mode will be;

$$\theta_{c5} = c\beta_s = \frac{\omega_b}{2\omega}(\beta_r - t) - \frac{\omega_b L_o I}{2V_s} \qquad (26)$$

The upper limit speed of this mode is the base speed.

MODE 4: *Speeds over than the base speed* $\omega > \omega_b$*:*

During this mode chopping no longer exists. The reduced negative period of mode 3 vanishes and incorporated into zero volt loop period. The switching sequence is summarised in table(4).

M \ S	S_a	D_a	S_b	D_b	S_c	D_c	S_e	D_e
1.	on	off	on	off	off	off	off	off
2.	off	on	on	off	on	off	off	off
3.	off	on	on	off	on	off	off	off
4.	off	on	off	on	on	off	on	off

Table(4). The switching sequence at $\omega > \omega_b$

During this mode each phase is exposed to *full positive* supply voltage during current rising (sub-mode 1), *zero voltage* during the conduction period of the next phase (sub-modes 2,3) and

finally *full negative* voltage after the conduction period of the next phase (sub-mode 4). The current-flux linkage loop is shown in figure(8). The flux linkage rise along OAB equals its fall along CDEO.

$$L_o I + V_s \frac{c\beta_s}{\omega} = \frac{\beta_r - t - c\beta_s}{\omega} V_s \qquad (27)$$

From which the commutation angle will be;

$$\theta_{c6} = c\beta_s = \frac{\beta_r}{2} - \frac{t}{2} - \frac{\omega L_o I}{2V_s} \qquad (28)$$

3.2. Motors with Five Phases and more:

These motors usually have rotor pole arc greater than two step angles. It is possible that the third phase starts while the first one still in duty. Similar to the first group, the commutation process can be categorized in one of the following four modes.

MODE 1: *Speeds below the first commutation speed* $\omega<\omega'_0$:

This mode is similar to that of the first group except that its upper speed limit is different. The commutation angle is given by eqn(15). The upper limit of this mode is the first commutation speed ω'_0. This limit is reached when the commutation angle is short enough such that the fall angle θ_f equals one step angle, that is;

$$\theta_f = t \qquad (29)$$

or;

$$\beta_r - c\beta_s = t \qquad (30)$$

Substituting the value of $c.\beta_s$ from eqn(30) in eqn(15) the first commutation speed for this category will be;

$$\omega'_o = \frac{\omega_b t}{\beta_r + \frac{\omega_b L_o I_m}{V_s}} \qquad (31)$$

MODE 2: *Speeds over or equal the first commutation speed and less than the second commutation speed* $\omega'_0<=\omega<\omega'_1$:

During this mode both θ_f and $c.\beta_s$ exceed one step angle. It is possible to apply the full negative supply voltage across the first phase just after the end of chopping period of the second phase. The switching sequence is summarised in the table(5).

During this mode each phase is exposed to *full positive* supply voltage during current rising (sub-mode 1), *reduced positive* during chopping (sub-modes 2,3), *reduced negative* voltage due to chopping in the next phase (sub-mode 4) and finally *full negative* voltage when chopping is no longer exist in the next phase (sub-mode 5).

M / S	S_a	D_a	S_b	D_b	S_c	D_c	S_e	D_e
1.	on	off	on	off	off	off	off	off
2.	chop	chop	on	off	on	off	off	off
3.	chop	chop	on	off	chop	chop	off	off
4.	off	chop	chop	chop	on	off	off	off
5.	off	on	off	on	chop	chop	on	off

Table(5). The switching sequence at $\omega'_0 <= \omega < \omega'_1$

The current-flux linkage loop is shown in figure(9). The flux linkage rise along OAB equals the flux linkage fall along BCO.

$$L_o . I + C . \psi_{max} = \frac{t}{\omega}\left(1 - \frac{\omega}{\omega_b}\right) V_s + \frac{\beta_r - t - c\beta_s}{\omega} V_s \qquad (32)$$

From which the commutation angle will be;

$$\theta_{c7} = c\beta_s = \frac{\omega_b\left(\beta_r - t\left(\frac{\omega}{\omega_b}\right) - \frac{\omega L_o I}{V_s}\right)}{(\omega + \omega_b)} \qquad (33)$$

The upper speed limit of this commutation angle is the second commutation speed ω'_1. It is the speed at which the commutation angle equals one step angle, that is;

$$c\beta_s = t \qquad (34)$$

Substituting this value in eqn(33) yields;

$$\omega'_1 = \frac{\omega_b(\beta_r - t)}{2t + \frac{\omega_b L_o I_m}{V_s}} \qquad (35)$$

MODE 3: *Speeds over or equal the second commutation speed and less than the base speed* $\omega'_1 <= \omega < \omega_b$:

This mode starts when the commutation angle becomes equal to one step angle. After this point a zero volt loop will exist until chopping starts in the next phase. It is similar to Mode 3 of the first group except that its upper speed limit is different. The commutation angle for this mode is given by eqn(26). The upper limit speed of this mode is the base speed.

It should be noted that depending on the rotor pole arc, this mode could be vanished. It is possible, in some motors, that the second commutation speed equals or exceeds the base speed. Eqn(35) can be rewritten in the form,

$$\frac{\omega'_1}{\omega'_b} = \frac{(\beta_r - t)}{2t + \frac{\omega_b L_o I}{V_s}} \qquad (36)$$

If the second commutation speed exceeds the base speed then the right hand side of eqn(36) should be greater than one. From which we can obtain the condition for this case,

$$\beta_r < \frac{\omega_b L_o I}{V_s} + 3t \qquad (37)$$

This case could exist for seven phases and more.

MODE 4: *Speeds over the base speed $\omega > \omega_b$:*

During this mode chopping no longer exists. This Mode is also the same like Mode 4 of the first group. The commutation angle for this mode is given by Eqn(28).

4. COMPUTER PROCEDURE TO PREDICT THE IDEAL COMMUTATION ANGLE:

The analysis given in section(3) are implemented in a computer procedure, Fig(10), to predict the ideal commutation angle for a certain running speed and machine data. This procedure is incorporated as a subroutine of another larger program to study the SRM performance and the interaction of the switching angles with the whole performance of the machine. The machine data given in Ref[8] are used herein to study the present analysis.

The ideal commutation angle is predicted with the procedure summarized in Fig(10) over a wide range of running speeds and shown in Fig(11). This angle always gets narrower with the increase of motor speed. It is of importance to note that the computer procedure uses different expressions, of those analytically obtained in section(3), to predict the commutation angle over different sub-speed ranges. This means the curve which represents the commutation angle is assembled of many portions, each one is obtained from the expression which is valid over its sub-speed range. This explains why this curve is not smooth over the whole range.

The rise angle θ_r, defined by Eqn(8), is always proportional to the running speed. This angle is also obtained over the same speed range and shown on Fig(11). Both rise and commutation angles *constitute the whole angle during which a positive volt pulse* should be applied across the phase winding.

$$\theta_v = \theta_r + \theta_c \qquad (38)$$

The variation of this angle with the speed is also given on Fig(11). There is an important notice which can be obtained from this curve. Although the commutation angle should always be reduced with the increased speed, this reduction has to be compensated by the rise angle and no much variation of the whole angle θ_v is required to get ideal commutation. In other words, both turn-on and turn-off points should continuously be readjusted such that they become earlier at higher speeds.

5. EXPERIMENTAL RESULTS:

From the former analysis, the SRM can be ideally commutated by continuously readjusting the turn-on and turn-off points with the motor speed. Since the whole angle θ_v does not change too much, an average value could be chosen to study the effect of advancing and retarding the voltage pulse with the speed. The analytical study is applicable to any number of phases, however it is intended to investigate the commutation and switching process of a multiphase SRM. A laboratory test rig is built for experimental verification of analytical results. This rig consists of a five-phase SRM [8], a compact power converter[9], and their essiential interface electronics. The integrated experimental rig is documented in another publication[10].

A constant voltage of pulse width $\theta_v=0.8\beta_s$ is used for experimental test. The torque-speed results are shown in figure(12), where the bold curve represents the characteristic for turn-on exactly at unaligned axis. The curves to the right of the first one are obtained with earlier turn-on angles measured from the unaligned axis. The curve shown to the left of the bold one is obtained with a delayed commutation. It is quite clear that the machine output performance is directly affected by changing the turn-on points. A wide range of characteristics can be obtained by changing the excitation turn-on point.

6. CONCLUSIONS:

An ideal excitation current waveform has been characterized to maximize the output torque of a multiphase SRM. The switching sequence has been analyzed and the ideal commutation angle is obtained for each running condition. A simple procedure has been given to predict this angle and incorporated in a larger computer program to study its interaction with whole performance of the machine. The analytical results have been experimentally tested on a five-phase SRM. It has been found that early excitation pulses greatly improve the machine performance at high speeds. A very wide range of characteristics is possible by advancing and retarding the converter pulses with respect to the rotor position.

7. LIST OF BASIC SYMBOLS:

c	Commutation ratio ($c=\theta_c/\beta_s$).
I	Current chopping level [amp].
L_0	Minimum phase inductance [henry].
R	Phase resistance [ohm].
t	Step angle [rad] & time [Sec].
V_s	Supply voltage [volt].
β_s	Stator pole arc [rad].
β_r	Rotor pole arc [rad].
θ_r	Rise angle of phase current pulse [rad].
θ_c	Commutation angle of phase current pulse [rad].
θ_f	Fall angle of phase current pulse [rad].
ω	Motor speed [rad/Sec]

ω_0 First commutation speed of the first motor group (Eqn.16)
ω_1 Second commutation speed of the first motor group (Eqn.22)
ω'_0 First commutation speed of the second motor group (Eqn.31)
ω'_1 Second commutation speed of the second motor group (Eqn.35)

8. REFERENCES:

[1] *P.J.Lawrenson, J.M.Stephenson, P.T.Bienkinsop, J.Corda and N.N.Fulton*, "Variable Speed Switched Reluctance Motors", Proc.,IEE Pt-B 1980, Vol 127, No 4, July 1980, PP 255-265

[2] *W.F.Ray and R.M.Davis*,"Inverter Drive for Doubly Salient Reluctance Motor: Its Fundamental Behaviour, Linear Analysis and Cost Implications", Electric Power Applications, Vol 2, No 6, December 1979, PP 185-193

[3] *Timothy J. Miller*,"Converter Volt-Ampere Requirements of the Switched Reluctance Motor DRIVE", IEEE Trans. on Industry Applications, Vol IA-21, No 5, Sept/Oct 1985, PP 1136-1144

[4] *Finch,J.W., Metwally,H.M.B. and Harris,M.R.*,"Switched Reluctance Motor Excitation Current: Scope for Improvement", 2nd International Conference on Power Electronics and Variable Speed Drives (PEVD), 24-26 November 1986, Birmingham, United Kingdom, PP 196-199

[5] *Chappel,P.H.*,"Winding Current in a Switched Reluctance Motor", IEE Pt-B 134 No 5, 1987, PP 277-283

[6] *Chappel,P.H.*,"Current Pulses in Switched Reluctance Motor", IEE Pt-B 135 No 5, 1988, PP 224-230

[7] *Pollock,C. and Williams,B.W.*,"The Design and Performance of a Multiphase Switched Reluctance Drive", European Conference on "Power Electronics and Applications, EPE", Aachen, Germany 1989, PP 29-32

[8] *Khater,M.M., Hassanein,A.A., El-Shanawany,M.M, and Williams,B.W.*,"Five-Phase Switched Reluctance Motor. Part 1: Design and Performance" Engineering Research Bulletin, Vol. 17, Part 1, 1994, Faculty of Engineering, Menoufiya University, EGYPT, PP 121-136

[9] *Khater,M.M., El-Shanawany,M.M., Hassanein,A.A. and Williams,B.W.*, "Five-Phase Switched Reluctance Motor. Part 2: Power Converter and Switching Control" Engineering Research Bulletin, Vol. 17, Part 1, 1994, Faculty of Engineering, Menoufiya University, EGYPT, PP 137-152

[10] *Khater,M.M., El-Shanawany,M.M., Hassanein,A.A., Green,T.C. and Williams,B.W.*,"An Integrated Five-Phase Switched Reluctance Motor Drive",Fifth International Conference on "Power Electronics and Variable-Speed Drives (PEVD)", 26-28 October 1994, London, UK, (Accepted for Publication).

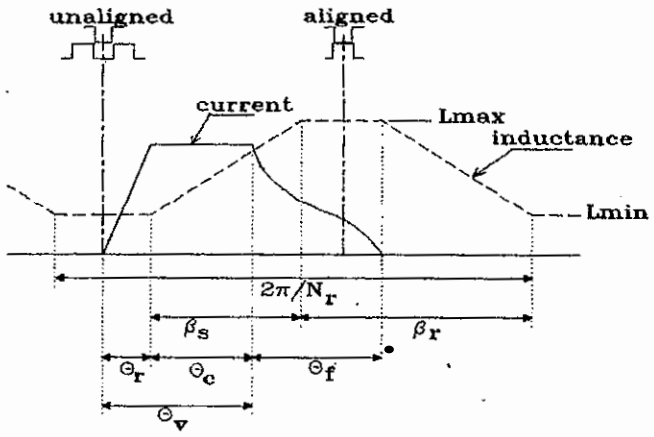

Figure 1. A typical phase current pulse along with the corresponding inductance profile.

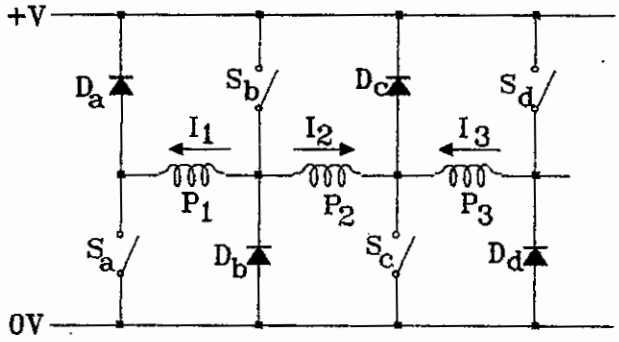

Figure 2. General section of the compact converter.

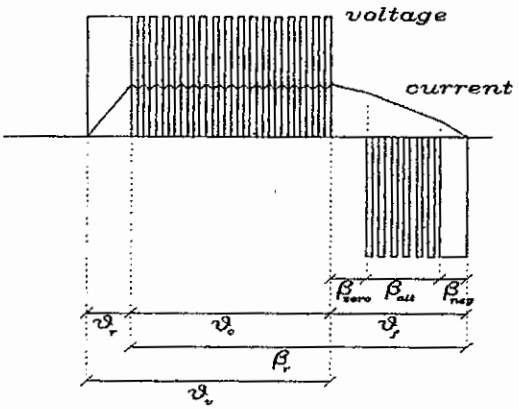

Figure 3 General voltage and current waveforms for the compact converter circuit under chopping.

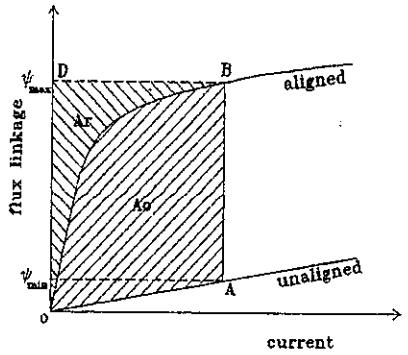

Figure 4. Current and flux linkage trajectory for one current pulse.

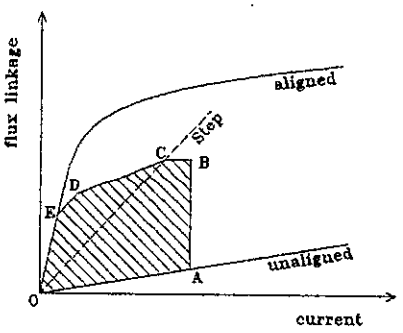

Figure 7. Current and flux linkage loop at $\omega_1 <= \omega < \omega_b$ or $\omega'_1 <= \omega < \omega_b$

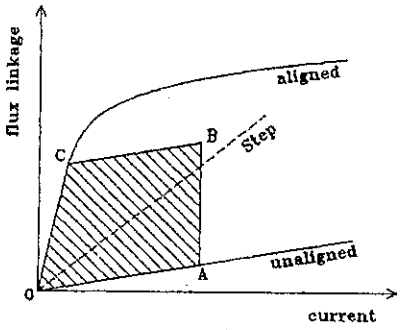

Figure 5. Current and flux linkage loop at $\omega < \omega_0$ or $\omega < \omega'_0$

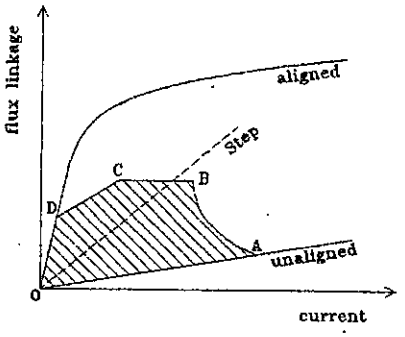

Figure 8. Current and flux linkage loop at $\omega > \omega_b$

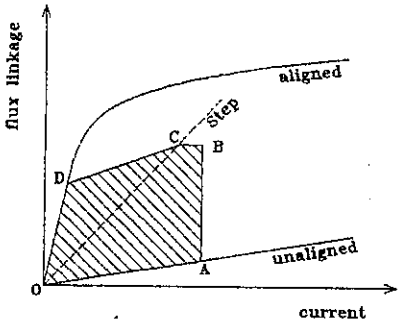

Figure 6. Current and flux linkage loop at $\omega_0 <= \omega < \omega_1$

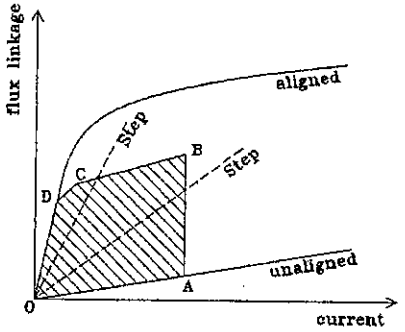

Figure 9. Current and flux linkage loop at $\omega'_0 <= \omega < \omega'_1$

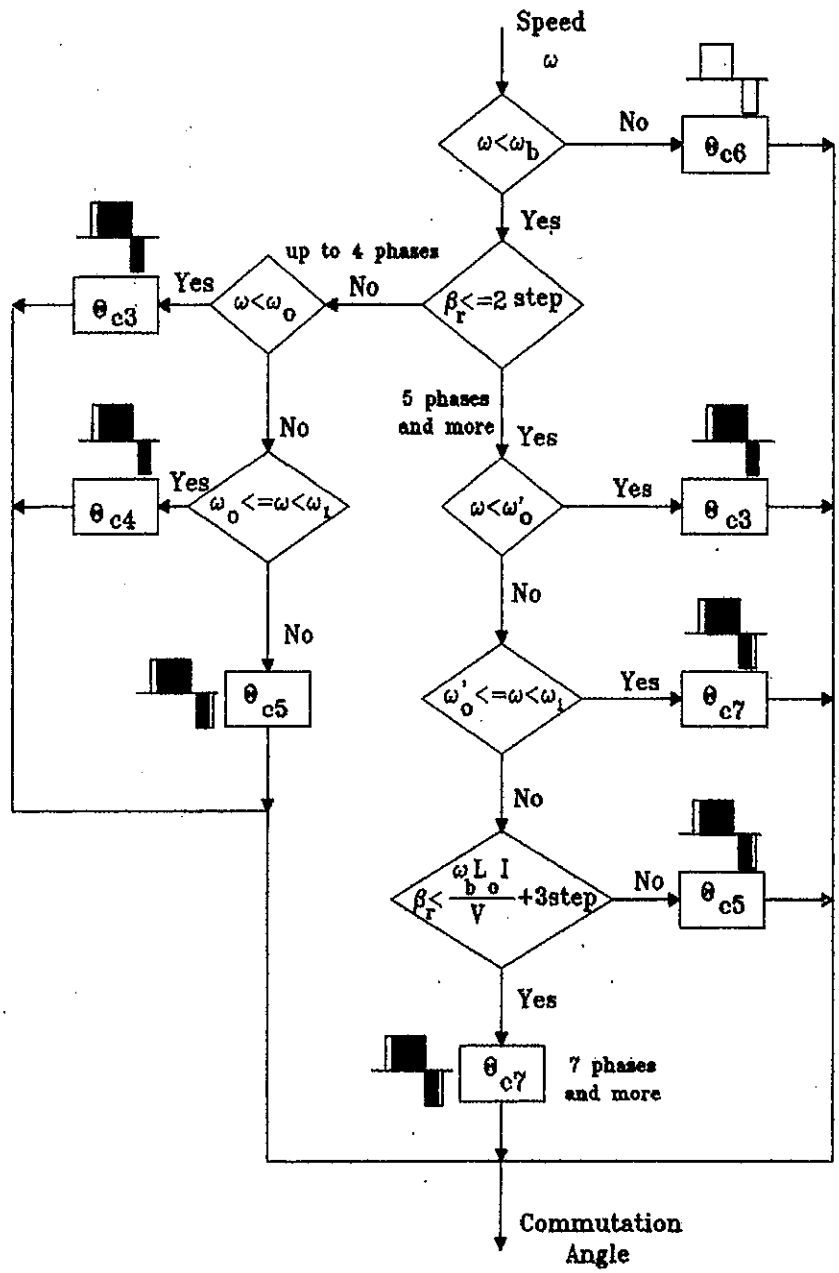

Figure 10. The procedure to predict ideal commutation angle.

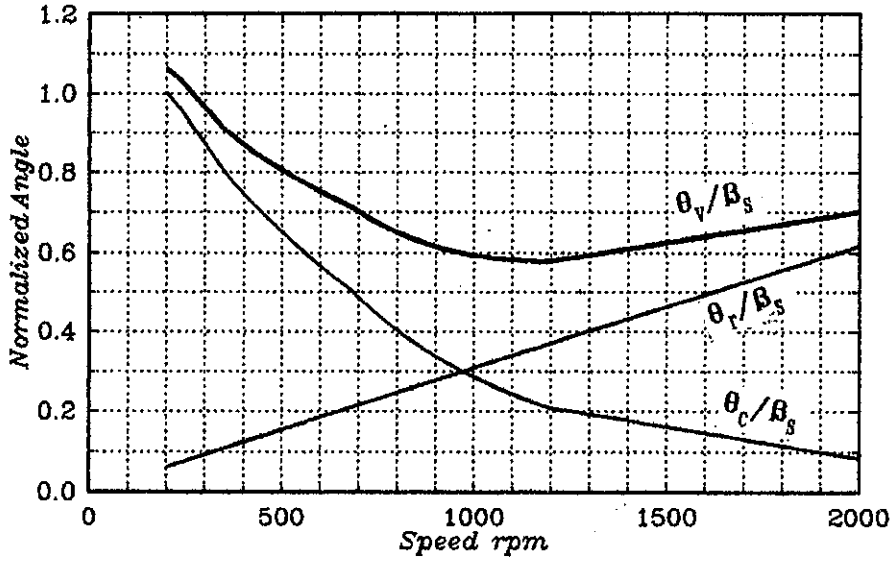

Figure 11. The variation of normalized rise angle (θ_r/β_s), commutation angle (θ_c/β_s) and positive volt angle (θ_v/β_s) with running speed Ref[10]

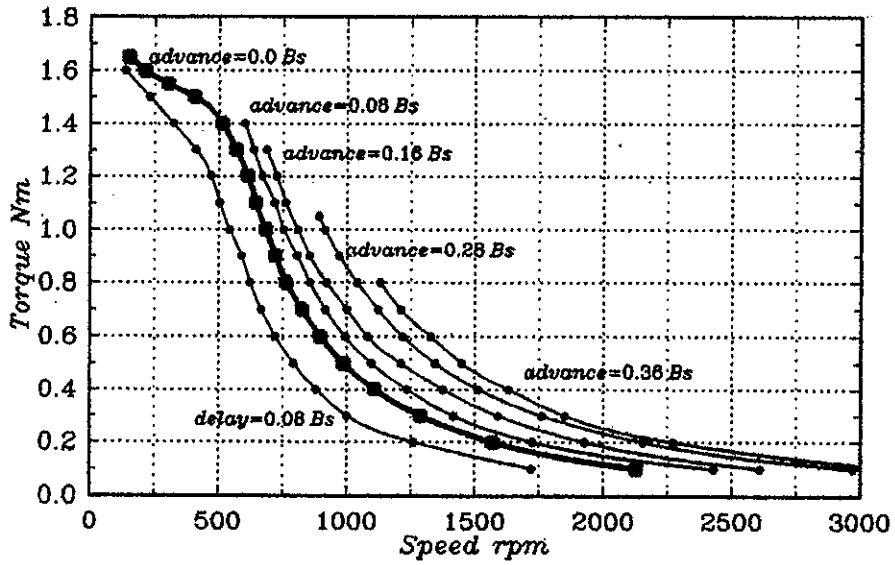

Figure 12. The experimental torque-speed characteristics for different turn-on points and constant positive volt pulse ($\theta_v=0.8\beta_s$)

المواصفات المثالية لنبضات تشغيل محرك الممانعة المغناطسية المتغيرة

تتناول هذه المقالة دراسة تحليلية وعملية لبحث المواصفات المثالية لنبضات التيار اللازمة لتشغيل محركات الممانعة المغناطيسية المتغيرة – عديدة الأوجه – عند قيم عظمى لعزم الحمل.

فى إطار هذه الدراسة تم تحليل نبضات تيار التغذية وحساب الزوايا المرحلية التى تتكون منها كل نبضة، ثم إستنتاج الشروط اللازم توفرها فى تلك المراحل للحصول على أقصى عزم من المحرك، بعد ذلك تم التوقف بالدراسة والتحليل عند المرحلة الرئسية من تلك النبضات وهى زاوية التبديل حيث تم بحث كافة المتغيرات التى يتوقف عليها مقدار تلك الزاوية عند ظروف التشغيل المختلفة، وأمكن صياغة العديد من الصور الرياضية لهذه الزاوية حسب سرعة التشغيل وبيانات المحرك، كما أمكن أيضا حساب شروط الحالات الإنتقالية بين مختلف تلك الصور الرياضية، ثم تم تلخيص تلك الصور الرياضية في أسلوب منهجي لإستنتاج قيمة تلك الزاوية، وتم برمجتة علي الحاسب الآلي وبفحص النتائج التحليلية تبين أن زاوية التبديل المثالية تتناسب عكسيا مع سرعة المحرك، إلا أن العرض الكلى لنبضة التغذية لايتغير كثيرا مع السرعة، حيث يتطلب التشغيل المثالى الإتيان المبكر لتلك النبضات.

من مجمل هذا الإستنتاج التحليلى تم إجراء عدة إختبارات معملية لإستنتاج خواص العزم والسرعة على منظومة محرك خماسى الأوجه، حيث تمت جميع الإختبارات بنبضات تغذية ذات عرض ثابت ولكن فى كل إختبار كانت زاويا بدء الإشعال مختلفة، وقد تبين من نتائج هذه الإختبارات المعملية صحة الإستنتاج التحليلى، حيث أدى الإشعال المبكر إلى تحسين ملحوظ في خصائص التحميل للمحرك خصوصا عند السرعات العالية.

تخلص هذه الدراسة إلى أنه يمكن الحصول على أقصى عزم تحميل من المحرك بإعادة الضبط المستمر للحظات إشعال نبضات التغذية مع تغير سرعة المحرك، كما يمكن أيضا الحصول على مدى كبير من هذه الخصائص فقط بتغيير تلك الحظات.